

# REPORT DOCUMENTATION PAGE

*Form Approved  
OMB No. 0704-0188*

Public reporting burden for this collection of information is estimated to average 1 hour per response, including the time for reviewing instructions, searching existing data sources, gathering and maintaining the data needed, and completing and reviewing this collection of information. Send comments regarding this burden estimate or any other aspect of this collection of information, including suggestions for reducing this burden to Department of Defense, Washington Headquarters Services, Directorate for Information Operations and Reports (0704-0188), 1215 Jefferson Davis Highway, Suite 1204, Arlington, VA 22202-4302. Respondents should be aware that notwithstanding any other provision of law, no person shall be subject to any penalty for failing to comply with a collection of information if it does not display a currently valid OMB control number. PLEASE DO NOT RETURN YOUR FORM TO THE ABOVE ADDRESS.

1. REPORT DATE (DD-MM-YYYY)		2. REPORT TYPE Technical Papers		3. DATES COVERED (From - To)	
4. TITLE AND SUBTITLE				5a. CONTRACT NUMBER  5b. GRANT NUMBER  5c. PROGRAM ELEMENT NUMBER	
6. AUTHOR(S)				5d. PROJECT NUMBER 2302 5e. TASK NUMBER MIGJ 5f. WORK UNIT NUMBER	
7. PERFORMING ORGANIZATION NAME(S) AND ADDRESS(ES)  Air Force Research Laboratory (AFMC) AFRL/PRS 5 Pollux Drive Edwards AFB CA 93524-7048				8. PERFORMING ORGANIZATION REPORT	
9. SPONSORING / MONITORING AGENCY NAME(S) AND ADDRESS(ES)  Air Force Research Laboratory (AFMC) AFRL/PRS 5 Pollux Drive Edwards AFB CA 93524-7048				10. SPONSOR/MONITOR'S ACRONYM(S)	
				11. SPONSOR/MONITOR'S NUMBER(S)	
12. DISTRIBUTION / AVAILABILITY STATEMENT  Approved for public release; distribution unlimited.					
13. SUPPLEMENTARY NOTES					
14. ABSTRACT					
15. SUBJECT TERMS					
16. SECURITY CLASSIFICATION OF:			17. LIMITATION OF ABSTRACT  A	18. NUMBER OF PAGES	19a. NAME OF RESPONSIBLE PERSON Leilani Richardson
a. REPORT Unclassified	b. ABSTRACT Unclassified	c. THIS PAGE Unclassified			19b. TELEPHONE NUMBER (include area code) (661) 275-5015

Standard Form 298 (Rev. 8-98)  
Prescribed by ANSI Std. Z39-18

*3k Separate files are enclosed*

1119 121

2302 M/62 TP-FY 99-0065

MEMORANDUM FOR PRR (Contractor Publication)  
*/In-House*

FROM: PROI (TI) (STINFO)

5 April 1999

SUBJECT: Authorization for Release of Technical Information, Control Number: AFRL-PR-ED-TP-FY99-0065  
Y. Kwon and C.T. Liu, "Damage in Particulate Composites with Hard Particles Embedded in a Soft Matrix"

12<sup>th</sup> International Conference on Composite Materials

(Statement A)

20021119121

# DAMAGE IN PARTICULATE COMPOSITES WITH HARD PARTICLES EMBEDDED IN A SOFT MATRIX

Young W. Kwon<sup>1</sup> and C. T. Liu<sup>2</sup>

<sup>1</sup> Department of Mechanical Engineering, Naval Postgraduate School  
700 Dyer Road, Monterey, California, 93943, USA

<sup>2</sup> Air Force Research Laboratory, AFRL/PRSM  
10 East Saturn Boulevard, Edwards AFB, California, 93524, USA

**SUMMARY:** Damage evolution in a particulate composite around a notch tip was studied. The composite had hard and stiff particles embedded in a soft and weak matrix like a rubber material. The major damage modes were the interface debonding called dewetting and the resulting matrix cracking because the particles were much stronger than the matrix. A numerical modeling and simulation of such damage was conducted using the micro/macro-approach. This technique combined micro-level analysis and macro-level analysis. Damage was described at the micro-level using a damage theory. Damage initiation and growth at a circular notch tip were predicted from the numerical study, and their results were compared ~~with~~ experimental data. Both results compared very well.

**KEYWORDS:** damage, particulate composite, micromechanics, finite element analysis, micro/macro-approach

## INTRODUCTION

Particle-reinforced composite materials have been 'used' widely in various engineering applications ranging from commercial applications to military applications. Their damage modes and mechanisms depend on properties of the reinforced particles, the binder matrix, and their interface. In general, the damage modes in a particulate composite are matrix damage (micro-cracking), interface debonding, and particle cracking. Relative strength and stiffness of the constituent materials and their interface including initial defects will govern the damage modes. The composite material under study has hard and strong particles embedded in a very soft and weak rubber-like matrix material. As a result, the major damage modes are interface debonding and matrix cracking [1]. In particular, the interface debonding called dewetting is the primary damage mode.

Previous research on these kind of composite materials has focused on material degradation based on damage evolution. Those studies attempted to develop macro-level constitutive

models incorporating progressive damages [2,3]. Other studies considered the progressive damage from notch tips [4-7]. Most of the previous studies did not consider dewetting explicitly. It was treated as a smeared damage in the composite [2-4] or in the matrix [5-7].

The objective of the paper is to model the progressive interface damage starting from a notch tip using a micro/macro-mechanical approach. The interface damage (dewetting) is considered explicitly at the micro-level analysis of the micro/macro-approach. The subsequent section describes the micro/macro-approach including the macro-level analysis, micro-level analysis, and a damage theory. Numerical results and discussion are presented next followed by conclusions.

### MICRO/MACRO-APPROACH

The modeling and simulation technique used in this study is called the micro/macro-approach [5-10]. The approach is similar to the local-global approach in structural analysis. The micro/macro-approach utilizes the two levels of analyses: micro-analysis and macro-analysis. The micro-analysis is performed at the constituent material level while the macro-analysis is undertaken at the composite structure level. The two analyses are conducted in tandem as damage initiates and evolves in composite structures. Damage is described at the micro-level in terms of the constituent materials. Damage modes for a particulate composite are described in terms of particle cracking, matrix micro-cracking, and interface debonding. The interaction between the two levels of analyses is shown in Fig. 1 and the description of each analysis is given below.

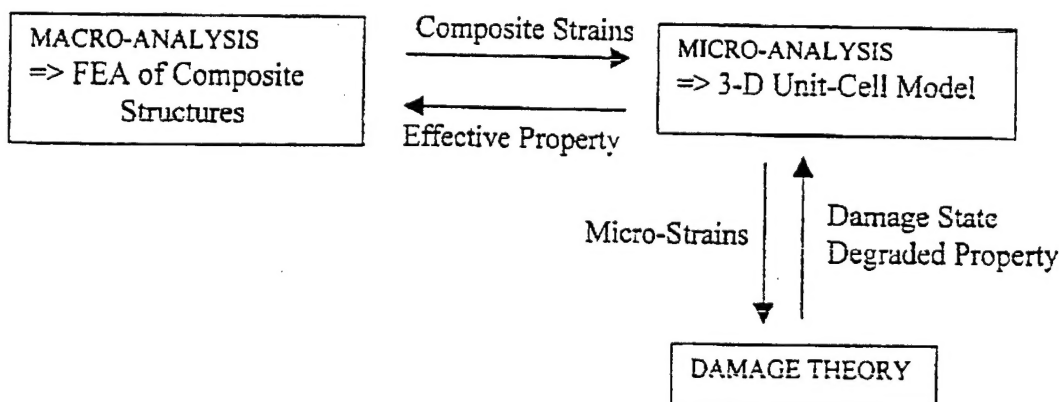


*Fig. 1: Interaction between micro-analysis and macro-analysis*

#### Macro-Analysis

The macro-analysis is conducted at the composite structure (specimen) level. Thus, the geometry and dimensions of the structure are at the macro-scale. For this level of analysis, any structural analysis technique can be adopted. However, in order to solve general cases of composite structures under diverse loading and boundary conditions, numerical solution techniques are suitable such as the finite element method [11-13], boundary element method [14,15], finite difference method [16], and meshless method [17]. Some combinations of these techniques may be used to take advantage of respective techniques. Because the finite element method has been most popular for structural analysis, it is used for the present study.

The composite structure under study is discretized into a finite element mesh with proper structural elements such as plate/shell, beam, 2-D continuum, and/or 3-D continuum elements. In general, isoparametric types of elements are used with the Gauss quadrature rule. These elements require material properties at the Gauss quadrature points. As a result, the interaction between the micro-analysis and the macro-level finite element analysis is performed at the Gauss quadrature points. The micro-analysis provides the Gauss quadrature points of the macro-analysis with effective composite material properties including the damage state. The macro-analysis is undertaken to compute deformation and stress/strain of the composite structure. These data are transferred to the micro-level analysis.

The present composite structure (specimen) to be studied is a square plate (76.2mm x 76.2 mm) with a through-the-thickness hole with diameter of 6.35mm at the center. Because of symmetry, a quarter of the plate is modeled. The specimen is subjected to a uniaxial tensile load. A uniform displacement ~~with~~ is applied to the edge of the specimen so that the numerical results can be compared to the experimental data.

### Micro-Analysis

Because the micro-analysis is conducted repeatedly at each Gauss quadrature point of respective finite element with iterative process as damage progresses, the analysis should be computationally efficient. To this end, a simplified analytical model is used for the micro-level analysis. One of them is a unit-cell model [18-22].

The micro-analysis has two major functions. One is to compute effective material properties of the composite based on the progressive damage ~~at~~ the constituent materials. These data are used for the subsequent macro-analysis. The other function is to decompose the macro-level stress/strain obtained from the previous macro-analysis into micro-level stress/strain. The micro-stress/strain is used to determine the damage state at the constituent material level. The continuum damage theory is utilized to describe the damage state as well as the degraded material properties of each constituent material. The micro-analysis utilizes the degraded material properties to calculate the updated material properties of the damaged composite.

The micro-model is shown in Fig. 2. It is a unit-cell consisting of eight sub-cells. The unit cell has dimensions of unity in every direction. One sub-cell (sub-cell 1 in Fig. 2) is the particle sub-cell and it is a cube ~~with~~ side length of  $(V_p)^{1/3}$  where  $V_p$  is the particle volume fraction of the composite. Then, sizes of the rest of sub-cells are determined accordingly. In order to model the particle/matrix interface debonding, linear springs are introduced at the interfaces of the particle sub-cell and three neighboring sub-cells. (The double arrows in Fig. 2 indicate linear springs at the interfaces) Before interface failure, the linear spring is very stiff. However, as interface damage called dewetting evolves in the model, the spring constant decreases accordingly. The amount of reduction in the spring stiffness is dependent upon the damage state. This will be discussed in the next section.

For mathematical simplicity that is an important part of the success of the micro/macro-approach in a practical sense, stress and strain are assumed to be uniform within each sub-cell. Then, stress equilibrium at the interface of any two neighboring sub-cells is enforced.

$$\sigma_{11}^1 = \sigma_{11}^2 \quad \sigma_{11}^3 = \sigma_{11}^4 \quad \sigma_{11}^5 = \sigma_{11}^6 \quad \sigma_{11}^7 = \sigma_{11}^8 \quad (1)$$

$$\sigma_{22}^1 = \sigma_{22}^3 \quad \sigma_{22}^2 = \sigma_{22}^4 \quad \sigma_{22}^5 = \sigma_{22}^7 \quad \sigma_{22}^6 = \sigma_{22}^8 \quad (2)$$

$$\sigma_{33}^1 = \sigma_{33}^5 \quad \sigma_{33}^2 = \sigma_{33}^6 \quad \sigma_{33}^3 = \sigma_{33}^7 \quad \sigma_{33}^4 = \sigma_{33}^8 \quad (3)$$

in which superscript denotes the sub-cell number as shown in Fig. 2 and subscript indicates the stress component. These equations are for normal components of stresses. Similar equations can be written for shear components but they are omitted here.

The deformations of sub-cells are assumed to satisfy the following relationship:

$$l_p \varepsilon_{11}^1 + l_m \varepsilon_{11}^2 + \left( l_p^2 \sigma_{11}^1 / k_1 \right) = l_p \varepsilon_{11}^3 + l_m \varepsilon_{11}^4 = l_p \varepsilon_{11}^5 + l_m \varepsilon_{11}^6 = l_p \varepsilon_{11}^7 + l_m \varepsilon_{11}^8 \quad (4)$$

$$l_p \varepsilon_{22}^1 + l_m \varepsilon_{22}^3 + \left( l_p^2 \sigma_{22}^1 / k_2 \right) = l_p \varepsilon_{22}^2 + l_m \varepsilon_{22}^4 = l_p \varepsilon_{22}^5 + l_m \varepsilon_{22}^7 = l_p \varepsilon_{22}^6 + l_m \varepsilon_{22}^8 \quad (5)$$

$$l_p \varepsilon_{33}^1 + l_m \varepsilon_{33}^5 + \left( l_p^2 \sigma_{33}^1 / k_3 \right) = l_p \varepsilon_{33}^2 + l_m \varepsilon_{33}^6 = l_p \varepsilon_{33}^3 + l_m \varepsilon_{33}^7 = l_p \varepsilon_{33}^4 + l_m \varepsilon_{33}^8 \quad (6)$$

where

$$l_p = V_p^{1/3} \quad (7)$$

$$l_m = 1 - l_p \quad (8)$$

Here,  $V_p$  is the particle volume fraction of the composite. In Eqs.(4)-(6),  $k_1$ ,  $k_2$ , and  $k_3$ , are spring constants in the respective interface as shown in Fig. 2. For isotropic damage, these constants are assumed to be the same.

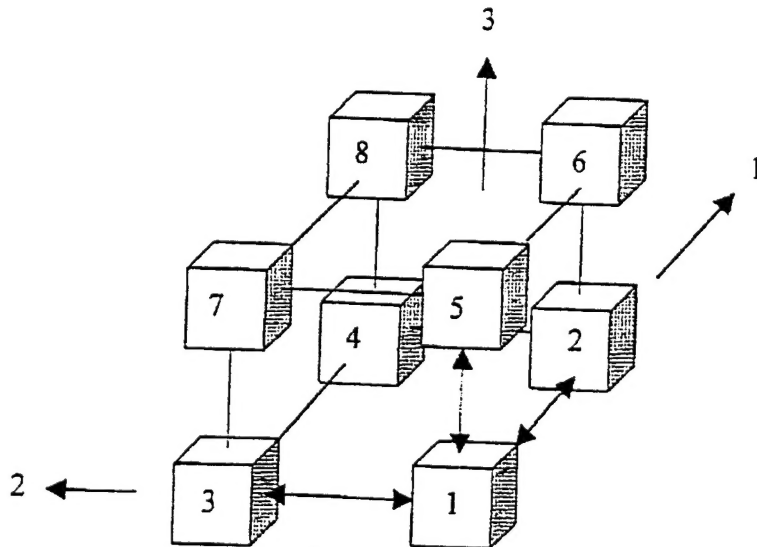


Fig. 2: Micro-model with eight sub-cells

Other necessary mathematical expressions are the constitutive equations for the particle and the matrix as well as for the composite. Furthermore, the composite stress and strain are assumed to be

$$\bar{\sigma}_{ij} = \sum_{n=1}^8 V^{ni} \sigma_{ij}^n \quad (9)$$

$$\bar{\varepsilon}_{ij} = \sum_{n=1}^8 V^{ni} \varepsilon_{ij}^n \quad (10)$$

where superimposed bar denotes the composite (macro) stress and strain, and  $V^n$  is the volume of the  $n^{\text{th}}$  sub-cell.

Algebraic manipulation of the previous equations finally yields the two key expressions as given below:

$$[\bar{E}^{\text{eff}}] = [V][E][R_2] \quad (11)$$

$$\{\bar{\varepsilon}\} = [R_2]\{\varepsilon^{\text{eff}}\} \quad (12)$$

in which  $[\bar{E}^{\text{eff}}]$  is the effective composite material property matrix,  $[V]$  is the matrix composed of sub-cell volume fractions,  $[E]$  is the matrix consisting of constituent material properties, and  $[R_2]$  is the matrix relating the sub-cell strain vector consisting of particle and matrix strains  $\{\varepsilon\}$  to the unit-cell strain vector (effective composite strain)  $\{\varepsilon^{\text{eff}}\}$ .

Equation (11) is used to compute the effective material properties of the composite material based on constituent material properties and their geometric information. Any degraded material property of the constituent materials associated with damage evolution is used to compute the effective property. Thus, this equation provides the connection from the micro-analysis to the macro-analysis. On the other hand, Eq. (12) provides the connection from the macro-analysis to the micro-analysis. That is, the equation decomposes the effective composite strains into micro-level strains at the particle and matrix. The micro-strains are used for the damage theory as described below to determine the progressive damage, and they are also used to compute micro-stresses.

### Continuum Damage Theory

Damage at the micro-level is described using a continuum damage theory. In general, an anisotropic damage theory can be applied to the constituent materials because the damage state may be anisotropic depending on the given conditions. An anisotropic damage theory, however, requires many material parameters most of which are not easily available. On the other hand, a simpler isotropic damage theory may be used at the micro-level assuming that each constituent material behavior is isotropic at the level and its damage state is also isotropic. These assumptions are realistic. Therefore, an isotropic damage theory is used in this study.

Because the interface debonding called dewetting is the major damage mode in the present composite, the present damage theory addresses this kind of damage. It is assumed that the damage growth at the interface is related to the change of the volume like

$$d\phi = (1-\phi)d\varepsilon_u \quad (13)$$

where  $\phi$  is the damage parameter and  $\varepsilon_u$  is the strain tensor of a material. This equation applies when an induced strain measure exceeds the threshold value which is material dependent. The damage expression is based on the experimental observation which showed that the volume dilatation increases as damage grows.

Once the damage parameter  $\phi$  is computed, the interface spring constant is adjusted based on the amount of the damage using

$$k = k_0 f(\phi) \quad (14)$$

in which  $k$  is the reduced interface spring constant and  $k_0$  is the original spring constant before interface damage. The function  $f$  is assumed as

$$f(\phi) = 10^{-c\phi} \quad (15)$$

where  $c$  is a material constant. Another kind of damage theory was used in Ref. 4 and 6.

## RESULTS AND DISCUSSION

First of all, the stress-strain behavior of a uniform specimen of the composite is plotted in Fig. 3. The experimental data are compared to the numerical data obtained from the micro/macro-approach. The two curves compare well until final fracture of the specimen. Damage initiation and growth is shown in Fig. 4. As seen in the figure, damage initiates at the applied strain level of a little less than 0.05 m/m, where Fig. 3 shows the deviation from the linear stress-strain curve. That is, damage initiation and growth result in nonlinear stress-strain behavior until fracture. The maximum value of damage parameter in Fig. 4 is considered as the saturation of damage.

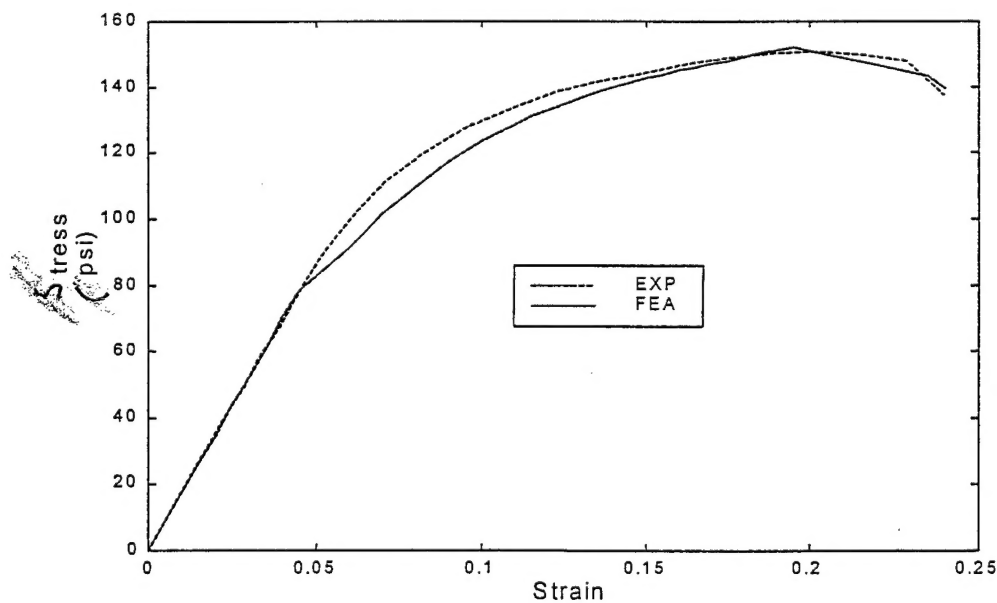


Fig. 3: Stress-strain curve of a uniform composite specimen

In general, damage growth in a uniform composite specimen is not uniform across the specimen because of non-uniform microstructures including non-uniform particle distribution in the composite. Thus, damage varies from point to point in the specimen. However, the analytical model cannot implement such a non-uniform variation. Instead, only the average damage in the composite can be simulated. As a result, a local maximum damage value in the composite specimen may be greater than the maximum value shown in Fig. 4. In the subsequent study, this maximum damage value is used as the damage saturation value and the percentage of damage is computed based on that maximum damage value.

The next example is a composite specimen with a through-the-thickness circular hole at the center of the specimen. The specimen geometry was provided in the previous section. The specimen is subjected to a uniform displacement along two opposite edges.

Figure 5 shows the plot of the applied strain versus the induced strain at the notch tip. The applied strain is computed from the applied displacement divided by the specimen length. The notch tip strain is the component along the loading direction. As expected, the induced strain at the notch tip is three times greater than the applied strain due to strain concentration at a low applied strain level. As damage initiates and grows at the notch tip, the material at the tip degrades. As a result, the induced strain increases greater than the applied strain. That is, the slope in Fig. 5 increases as damage grows. The crack tip strain compares well with the experimental observation. Because of a high strain value at the notch tip, the experiment could not measure the notch tip strain directly. Instead, the strain a little distance away from the notch tip was measured and extrapolated to the notch tip for comparison.

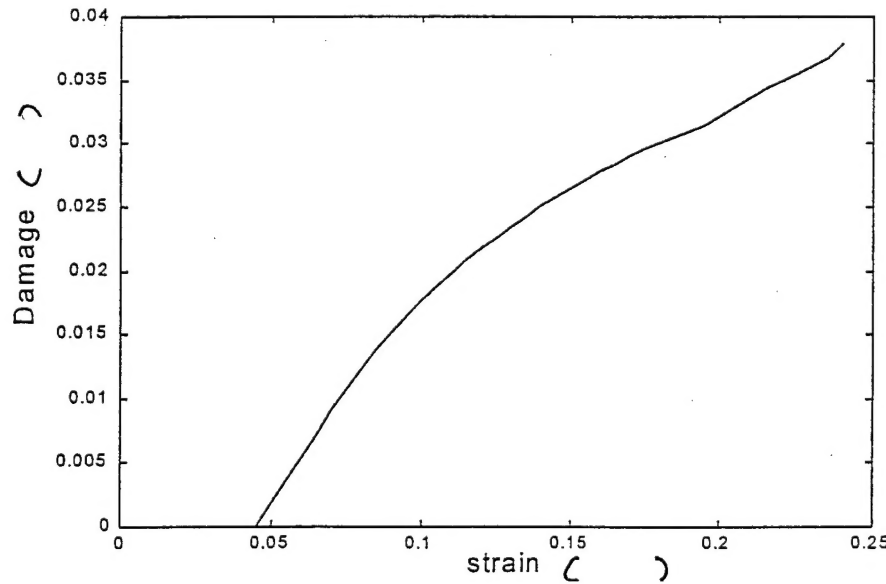


Fig. 4: Damage growth in a uniform composite specimen

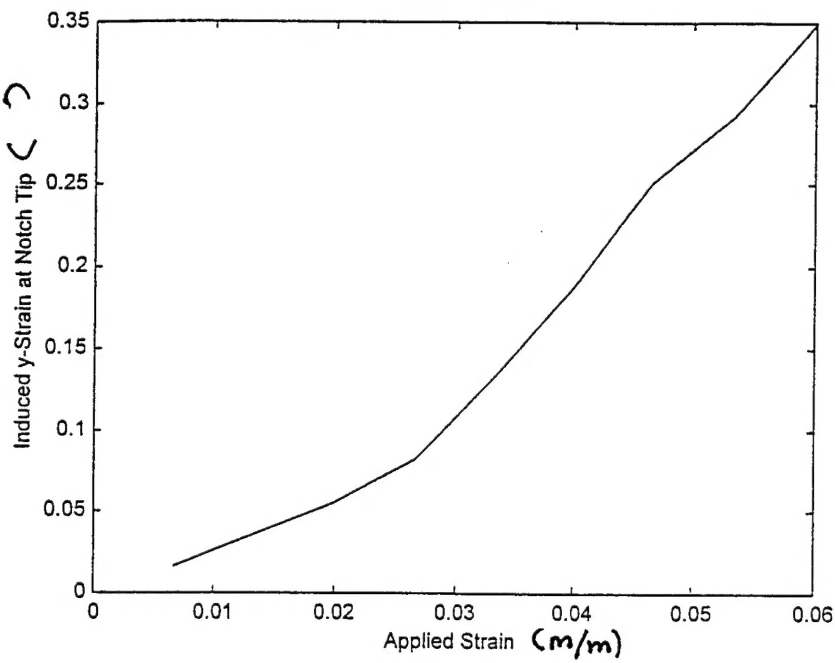


Fig. 5: Plot of induced notch tip strain versus applied strain

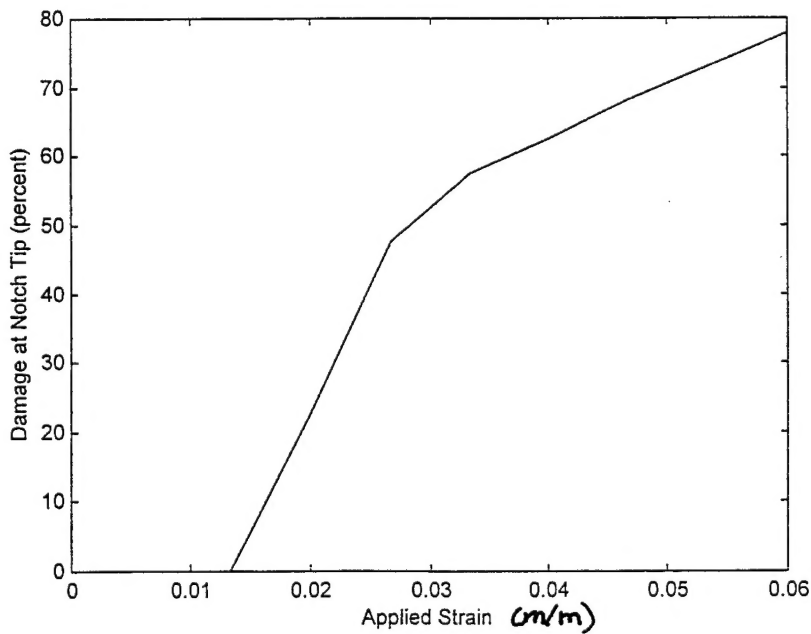


Fig. 6: Plot of damage at the notch tip vs. applied strain

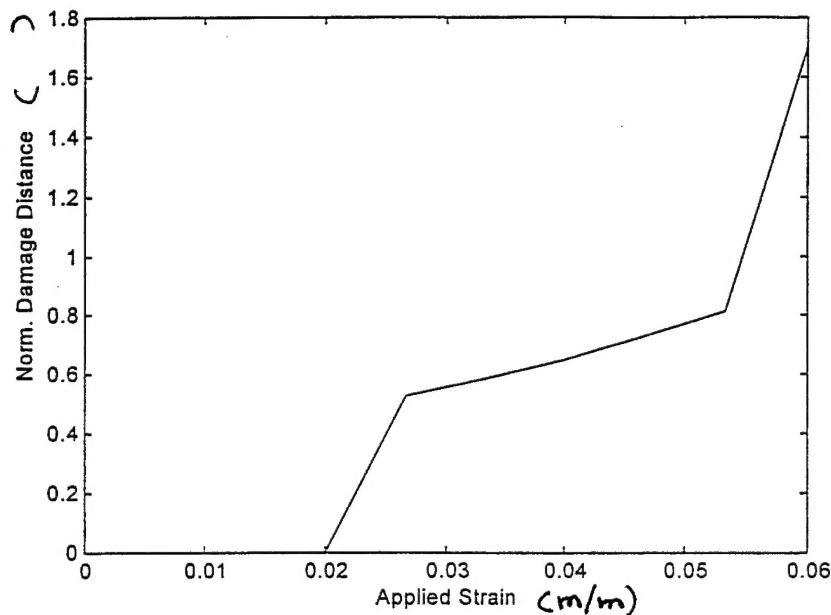


Fig. 7: Normalized damaged distance from the notch tip as a function of the applied strain

Figure 6 plots the damage initiation and growth at the crack tip. The damage at the notch tip begins at the applied strain of 0.012 m/m. Just after damage initiation, the damage growth rate (defined as damage increase per applied strain) is almost linear for a while and the rate decreases as the applied strain increases further.

Figure 7 shows the distance from the notch tip where the induced damage reaches more than 50 percent of the maximum value. The distance was normalized with respect to the hole diameter. The plot indicates that the damage growth along the minimum section of the perforated specimen is not linear. That is, damage growth direction varies along with the applied strain. [The major damage growth is approximately in the 45 degree from the applied loading direction from the notch tip.]

## CONCLUSIONS

The micro/macro-approach was applied to model and simulate damage initiation and growth in a particulate composite which consisted of hard and stiff particles and a soft and weak rubber-like matrix. The major damage mode called dewetting was modeled at the micro-level using interface springs and a damage theory. The numerically predicted stress-strain curve of the composite and the notch tip strain including damage compared well with experimental data. The micro/macro-approach can be used to predict the strength of a notched composite strength.

16. Forsythe, G.E. and Wasow, W.R., *Finite Difference Methods for Partial Differential Equations*, John Wiley & Sons, New York, 1960.
17. Belytschko, T., Krongauz, Y., Organ, D., Fleming, M., Krysl, P., "Meshless Method: An Overview and Recent Development", *Computer Methods in Applied Mechanics and Engineering*, Vol. 139, 1996, pp. 3-47.
18. Aboudi, J., "Closed Form Constitutive Equations for Metal Matrix Composites", *Int. J. Engineering Science*, Vol. 25, No. 9, 1987, pp. 1229-1240.
19. Aboudi, J., "Micromechanical Analysis of Composites by the Method of Cells", *Applied Mechanics Review*, Vol. 42, No. 7, July 1989, pp. 193-221.
20. Kwon, Y.W. and Byun, K.Y., "Development of a New Finite Element Formulation for the Elasto-Plastic Analysis of Fiber-Reinforced Composites", *Computers & Structures*, Vol. 35, No. 5, 1990, pp. 563-570.
21. Kwon, Y.W., "Calculation of Effective Moduli of Fibrous Composites with Micro-Mechanical Damage", *Composite Structures*, Vol. 25, pp. 187-192.
22. Kwon, Y.W. and Kim, C., "Micromechanical Model for Thermal Analysis of Particulate and Fibrous Composites", *Journal of Thermal Stresses*, Vol. 21, 1998, pp. 21-39.